A Novel Iron-Chelating Derivative of the Neuroprotective Peptide NAPVSIPQ Shows Superior Antioxidant and Antineurodegenerative Capabilities

Dan Blat,[†] Lev Weiner,[‡] Moussa B. H. Youdim,[§] and Mati Fridkin*,[†]

Department of Organic Chemistry and Department of Chemical Research Support, Weizmann Institute of Science, Rehovot, Israel, and Eve Topf and U.S.A. National Parkinson Foundation Centers for Neurodegenerative Diseases and Department of Pharmacology, Faculty of Medicine, Technion, Haifa, Israel

Received July 4, 2007

Affecting an estimated 5% of adults over 65 years of age, Parkinson's disease and Alzheimer's disease are the most common neurodegenerative disorders. Accumulating evidence suggests that oxidative stress induced by the breakdown of iron homeostasis is a major contributor to the neuronal loss observed in neurodegeneration. Thus, brain-permeable iron chelators may present potential therapeutic benefits. In the present study, iron-chelating hydroxamate groups were introduced into the NAP (NAPVSIPQ) peptide, whose neuroprotective qualities have been widely demonstrated. Our experiments revealed that the novel dihydroxamate peptide **3** is capable of inhibiting iron-catalyzed hydroxyl radical formation and lipid peroxidation, abilities that are not part of the repertoire of its parent peptide. In addition, peptide **3** was superior to native NAP in protecting human neuroblastoma cell cultures against the toxicity of hydrogen peroxide. These results suggest that NAP-based iron chelators deserve further investigation in the search for drug candidates for neurodegeneration.

Introduction

Alzheimer's disease (AD) and Parkinson's disease (PD) are the two most common forms of neurodegeneration. To date, no satisfactory treatment has been introduced for these neurodegenerative disorders, with present drugs offering symptomatic benefits at best. This unfortunate reality is at least in part attributable to a rather limited understanding of the etiological basis of neurodegeneration. Nevertheless, research in the past 2 decades has made it apparent that both oxidative stress and deposition of disease-specific protein aggregates are highly recurring motifs in neurodegenertion.[1,2] Evidence for the role of oxidative stress is based, among others, on abnormally high amounts of oxidatively modified proteins, lipids, and DNA in the brains of patients.[3–7]

Much of the work concerning the pathological oxidative processes observed in AD and PD has been devoted to the involvement of iron ions.[8] Studies in rodents have shown that normal aging is accompanied by a rise in the levels of iron and other metals (e.g., copper, zinc) in the brain.[9,10] These findings were complemented by post-mortem human brain tissue analyses, which revealed that the age-related iron increase occurs mostly in neurodegeneration-prone regions such as the substantia nigra, cortex, and hippocampus.[8] High content ($10^{-4}-10^{-3}$ M range) iron deposits are found in the abnormal protein aggregates typical of neurodegenerative brains: β-amyloid peptide (Aβ) plaques[11,12] and neurofibrillary tangles[12] in the case of AD and α-synculein (Lewy bodies)[13] in PD. Iron has been found to be involved in several key pathogenic processes in neurodegeneration:

(1) Redox-active Fe(II) reacts with H_2O_2 to generate the highly reactive $^{\bullet}$OH (hydroxyl radical) via the Fenton reaction Fe(II) + H_2O_2 → Fe(III) + OH^- + $^{\bullet}$OH.[14,15]

(2) Both Aβ[16] and α-synuclein[17] have been reported to generate H_2O_2 from molecular oxygen via electron transfer interactions involving bound redox-active Fe(III).

(3) Iron and other metals (copper, zinc) have been shown to promote fibrillation and aggregation of the Aβ peptide[18,19] and of α-synuclein.[20]

(4) Translation of the amyloid precursor protein (APP[a]), which is the parent protein of Alzheimer's Aβ peptide, is upregulated in the presence of iron.[21] This finding, together with the notion that high protein concentrations promote misfolding and aggregation,[2] points to yet another potential role for iron in neurodegeneration.

Thus, iron provides an interesting and potentially critical link between oxidative stress and deposition of protein aggregates. This apparently crucial role of iron suggests that chelating agents may possess therapeutic potential. Such compounds should be able to sequester free redox-active iron from its sites of activity, forming nontoxic metal complexes that are then excreted. Several compounds have been studied in the past in this context, including the prototype iron chelator drug desferrioxamine (DFO) and the orally available antibiotic clioquinol (5-chloro-7-iodo-8-hydroxyquinoline). Both these drugs showed potent neuroprotective capabilities in several cell culture and animal models for neurodegeneration.[22–25] However, neither has been successfully introduced for clinical use, for reasons of toxicity

* To whom correspondence should be addressed. Phone: +972-(0)8-9342505. Fax: +972-(0)8-9344142. E-mail: mati.fridkin@weizmann.ac.il.

[†] Department of Organic Chemistry, Weizmann Institute of Science.

[‡] Department of Chemical Research Support, Weizmann Institute of Science.

[§] Eve Topf and U.S.A. National Parkinson Foundation Centers for Neurodegenerative Diseases and Technion.

[a] Abbreviations: ADNP, activity-dependent neuroprotective protein; APP, amyloid precursor protein; Boc, *tert*-butyloxycarbonyl; DCC, dicyclohexylcarbodiimide; DCM, dichloromethane; DFO, desferrioxamine; DIPEA, diisopropylethylamine; DMF, *N*,*N*-dimethylformamide; EPR, electron paramagnetic resonance; Fmoc, 9-fluorenylmethoxycarbonyl; HOBt, *N*-hydroxybenzotriazole; LPO, lipid peroxidation; MDA, malondialdehyde; MTT, 3-(4,5-dimethylthiazol-2-yl)-2,5-diphenyltetrazolium bromide; NMM, *N*-methylmorpholine; NMP, *N*-methyl-2-pyrrolidone; Ofm, *O*-fluorenylmethyl; PBN, phenyl-*tert*-butylnitrone; PyBOP, benzotriazol-1-yloxytripyrrolidinophosphonium hexafluorophosphate; ROS, reactive oxygen species; TBA, thiobarbituric acid; TES, triethylsilane; TFA, trifluoroacetic acid.

10.1021/jm070800l CCC: $40.75
Published on Web 12/14/2007

as well as poor bioavailability in the case of DFO.[26] More recently, the neuroprotective potential of additional chelating agents has been investigated; VK-28, a brain permeable hydroxyquinoline derivative, showed potent protection against 6-hydroxydopamine (6-OHDA) induced lesion in rats.[27] Epigallocatechin 3-gallate (EGCG), a component of green tea extracts whose antioxidant and metal-chelating activities are well established, showed neuroprotective activity in a 1-methyl-4-phenyl-1,2,3,6-tetrahydropyridine (MPTP) mouse model for PD,[28] as well as capacity to down-regulate APP and Aβ in cell cultures.[29]

Another potential therapeutic strategy in neurodegenerative disorders may be based on neuropeptides and their analogues. One such example is the NAP octapeptide, whose competence in counteracting many of the phenomena associated with neurodegeneration has been widely studied.[30,31] NAP (Asn-Ala-Pro-Val-Ser-Ile-Pro-Gln) was identified as the active element of activity-dependent neuroprotective protein (ADNP), a glial cell mediator of vasoactive intestinal peptide (VIP) induced neuroprotection.[32] Since its discovery, NAP has been shown to possess potent neuroprotective qualities both in cell cultures[33,34] and in animal models.[32,35] Most importantly, NAP has been detected in the brains of treated animals following intravenous administration, implying capability to cross the blood−brain barrier.[35,36]

The work presented here is part of an extensive ongoing endeavor aiming to combine the antineurodegenerative traits of two or more drugs into a single molecule. The concept of such bi- and multifunctional drugs arose from the recognition that neurodegeneration may be too complex and multifaceted for a single drug to offer complete and lasting benefits to patients. Several bifunctional compounds have demonstrated a potential for neuroprotection and disease modification.[37,38] One such example is M30, a conjugate of the iron chelator VK-28 and propargylamine, the molecular moiety responsible for the monoamine oxidase B-inhibiting activity of the anti-Parkinsonian drug rasagiline.[37,38]

In the present study, the NAP peptide was synthesized and chemically modified to confer it with iron-binding capabilities. We have previously shown that a NAP derivative containing an 8-hydroxyquinoline metal binding moiety possesses antioxidative and in vitro neuroprotective effects.[39] Here, we chose the hydroxamate group (CONHOH) as the iron-chelating moiety. It is well established that hydroxamates are powerful bidentate iron coordinators, and in fact, the prototype chelator DFO is a naturally occurring trihydroxamate siderophore.[40] Ye et al. have previously introduced hydroxamates into peptides as a means to achieve conformational rigidity through iron coordination.[41] Neuropeptide-based metal chelators may be targeted toward their respective loci and exert their significant therapeutic activity in various forms of neurodegeneration. This effect may be amplified by the intrinsic capacity of the peptide carrier. Thus, one or two hydroxamate groups were strategically placed in the NAP peptide sequence to keep the resulting derivatives as similar to the native peptide as possible. The iron-chelating, antioxidative and in vitro neuroprotective activities of these peptides were studied and compared to those of the native NAP peptide and DFO.

Results and Discussion

Peptide Design and Synthesis. In attempt to confer the NAP peptide with metal-chelating capabilities, we chose to introduce into it the iron-binding hydroxamate groups. Hydroxamate-based chelators, like other compounds that employ oxygen atoms as ligands, favor Fe(III) over Fe(II). Such compounds are much more selective toward iron as a whole, since Fe(II)-favoring chelators are also capable of binding other bioactive bivalent metals such as Cu(II) and Zn(II), implying that their use entails lower specificity and greater toxicity.[26,42] In addition, high-affinity Fe(III) chelators can bind Fe(II) ions and rapidly autoxidize them to Fe(III).[43,44] Thus, Fe(III)-favoring chelators practically bind both types of iron ions under most physiological conditions.

The sites on the NAP sequence modified into hydroxamates were either the backbone C-terminal glutaminyl carboxyl group (peptide **1**, H_2N-Asn-Ala-Pro-Val-Ser-Ile-Pro-Gln-CONHOH) or the side chain of the N-terminal asparagine (peptide **2**, H_2N-Asp(CONHOH)-Ala-Pro-Val-Ser-Ile-Pro-Gln-OH), or both (peptide **3**, H_2N-Asp(CONHOH)-Ala-Pro-Val-Ser-Ile-Pro-Gln-CONHOH) (Scheme 1). The selection of these sites was based on several factors, including minimal alterations to the native sequence and a previous finding that the integrity of the Ser-Ile-Pro region within NAP is crucial for its neuroprotective activity.[45] In addition, the two hydroxamates in peptide **3** were adequately far apart to allow two hydroxamates from one peptide molecule to bind the same iron ion.

Following synthesis, peptides were purified by HPLC (>99% by analytical HPLC) and subjected to amino acid analysis and mass spectrometry: native NAP, *m/z* 825.30, calcd 824.92; **1**, *m/z* 840.08, calcd 839.94; **2**, *m/z* 840.80, calcd 840.92; **3**, *m/z* 855.97, calcd 855.94. Overall yields ranged from ~25% for hydroxamated peptides to ~60% for nonmodified peptides.

Formation of Peptide−Fe(III) Complex. Spectrophotometric studies were conducted to evaluate the formation and the composition of peptide−Fe(III) complexes. The formation of complexes of organic ligands with transition metal ions can result in appearance of new absorbance peaks or shifting/disappearance of pre-existing ones. The results of our studies suggest that NAP hydroxamates, but not the native NAP peptide, form stable complexes with Fe(III) in water (pH 5) at room temperature. As shown in Figure 1, the addition of $FeCl_3$ to native NAP did not result in any significant changes in the 200–700 nm absorption spectrum other than a peak around 280 nm that is attributed to the $Fe(OH)_n$ adducts formed under these conditions. In contrast, addition of $FeCl_3$ to either monohydroxamate or dihydroxamate NAP derivatives led to appearance of a broad new peak with a maximum at 464 nm (Figure 1), indicative of Fe(III) complex formation. As expected, none of the peptides tested showed complex formation with either copper or zinc under a similar experimental setting (not shown). In order to estimate the stability of the peptide **3**−Fe(III) complex, the molar extinction coefficient at 464 nm was calculated as $\epsilon_{464} = 1480\ M^{-1}\ cm^{-1}$ from the absorbance of a solution containing a large excess (×10) of peptide **3** over iron, allowing for the assumption that in this scenario the complex concentration is very close to the initial iron concentration. Following this, the absorbance was measured at several peptide **3** and iron concentrations, and the stability constant was extracted as log $K \approx 4$.

In theory, the tetradentate peptide **3** can form a variety of complexes with the six coordinates of the iron ion, with different peptide to Fe ratios. In order to elucidate the stoichiometry of **3** binding to iron, the absorption spectrum of the peptide was measured with increasing concentrations of $FeCl_3$. Figure 2A indicates that under the experimental conditions a complex with a 1 to 1 (peptide **3** to Fe) molar ratio was formed. This finding was reinforced by mass spectrometry analysis of the complex, which gave a value of *m/z* 909.63, corresponding to 1 to 1

Scheme 1. Synthesis of Peptide **3**[a]

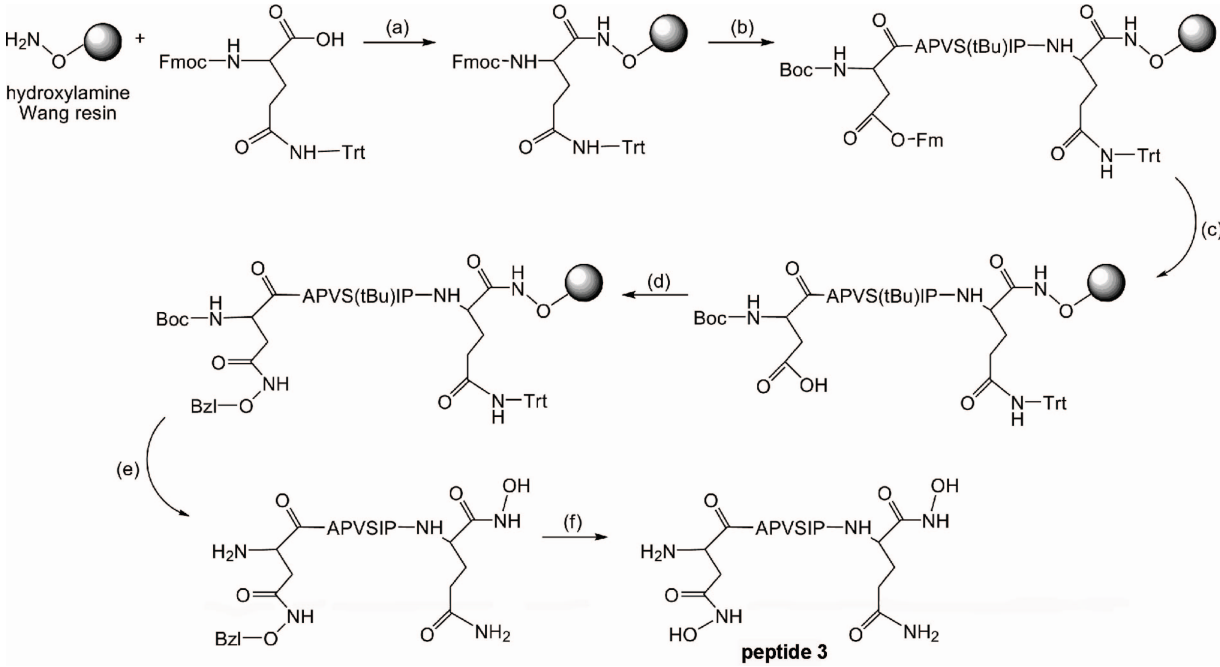

[a] (a) PyBOP, DIPEA. (b) Coupling: PyBOP, NMM. Fmoc-deprotection: 20% piperidine. (c) 20% piperidine; (d) *O*-benzylhydroxylamine + PyBOP and NMM (two cycles); *O*-benzylhydroxylamine + DCC and HOBt (one cycle); (e) TFA/triethylsilane (95:5); (f) 10% Pd/C, 1 atm of H_2.

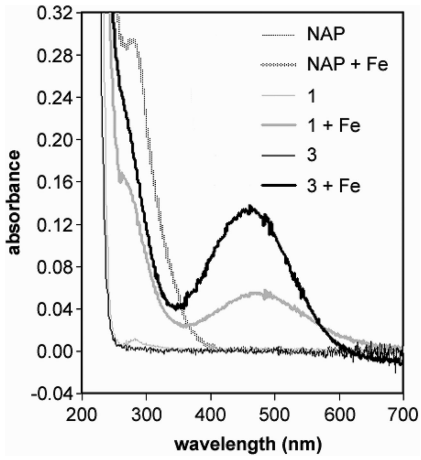

Figure 1. Spectrophotometric detection of peptide−Fe(III) complex formation. Absorption spectra of different NAP derivatives (0.3 mM) in the absence and presence (0.3 mM) of $FeCl_3$ in water.

stoichiometry (Figure 2B). It is our belief that in this complex the iron is coordinated by both hydroxamates of peptide **3** in a manner that can be described as iron-assisted cyclization.

Fe(II)-Chelating Potency. The Fe(II)-chelating potency of NAP and its hydroxamated derivatives was assessed by the ferrozine method. Binding of Fe(II) ions to ferrozine generates a colored complex that can be measured quantitatively at 562 nm.[46] The addition of iron chelators interferes with the ferrozine−Fe(II) complex in a concentration-dependent manner. Since high-affinity Fe(III) chelators bind Fe(II) ions and rapidly autoxidize them to the corresponding stable Fe(III) complex,[44] this method actually reflects the overall Fe(II)/(III)-chelating potency rather than affinity toward any of the two oxidation states. As expected, DFO, a very strong iron chelator (log K = 30.6 for Fe(III),[47] 10.3 for Fe(II)[48]), showed high iron-chelating potency, with an IC_{50} of 10 μM (not shown). The native NAP peptide did not exhibit any significant iron-chelating potency, while its hydroxamated derivatives were able to displace iron from ferrozine, with **3** showing higher chelating potency than **1** and **2** (peptides **1** and **2** IC_{50} = 360 μM, peptide **3** IC_{50} = 170 μM) (Figure 3).

DFO is one of ~500 identified naturally occurring siderophores, low molecular weight chelating agents that are produced by microbes in order to mediate uptake of the iron essential for their survival. Siderophores can acquire iron bound to other compounds through ligand exchange reactions.[49] Evidently, herein lies one of the adverse consequences of prolonged treatment with DFO: its extremely high affinity toward iron is believed to result in abstraction of the metal from its endogenous ligands (e.g., transferrin, log K = 20),[50] which can eventually lead to systemic iron depletion.[51] Thus, the lower affinity of the hydroxamated NAP peptides may have its merits in this respect, and it is possible that their chelating activity in vivo will be more selective toward free iron.

Inhibition of Lipid Peroxidation. Lipid peroxidation (LPO) is one of the major outcomes of oxidative stress-associated tissue damage. Since both AD and PD have been associated with elevated brain levels of lipid peroxidation products,[3,4] we have decided to employ an in vitro assay in order to examine the ability of NAP hydroxamates to inhibit iron/ascorbate-induced LPO. This widely used method is based on the oxidation of polyunsaturated fatty acids in biological membranes, giving rise to a variety of lipid breakdown products such as malondialdehyde (MDA). The reaction of MDA with thiobarbituric acid (TBA) forms a pink pigment that can be detected by visible light spectroscopy.

As can be seen in Figure 4, of the peptides tested **3** was the only one to possess an inhibitory effect against LPO, with an IC_{50} of 340 μM. Neither the monohydroxamate peptides nor the native NAP peptide had any antioxidative effect in this model, and in fact, at concentrations of 100 μM and higher, these peptides seem to increase lipid peroxidation in the presence of iron (Figure 4). The possibility that these peptides somehow enhance the MDA−TBA reaction was ruled out because no increase in the absorbance at 532 nm was detected when iron

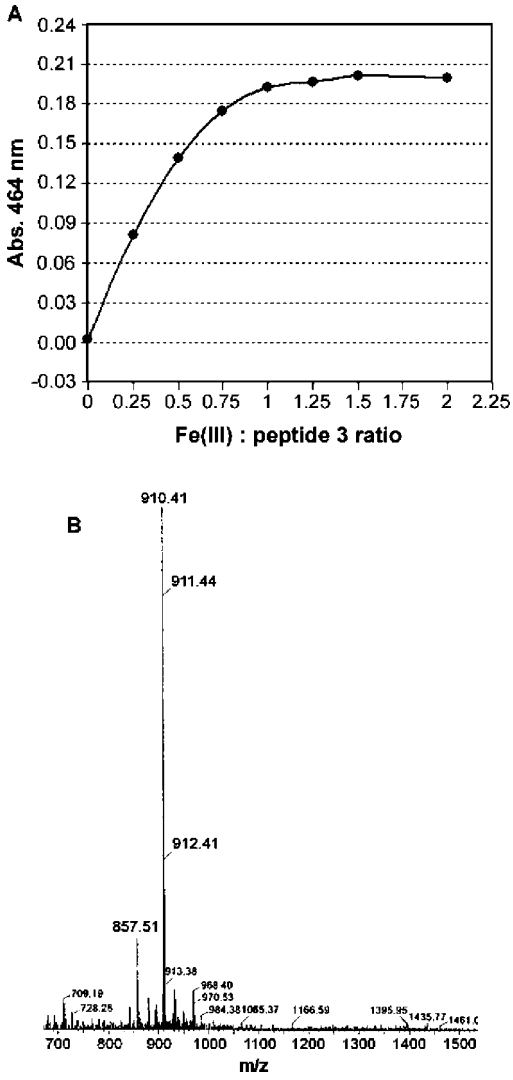

Figure 2. Stoichiometry of peptide **3**−Fe complex. (A) The absorption spectrum of peptide **3** (300 μM) in water was measured with increasing concentrations of $FeCl_3$. The absorbance at 464 nm saturates at approximately 300 μM $FeCl_3$, implying 1:1 binding stoichiometry. (B) Positive ion mass spectrum of peptide **3**−Fe complex, corresponding to 1:1 stoichiometry (calculated MW, 909.76). The peak at *m*/*z* 857.51 corresponds to peptide **3**.

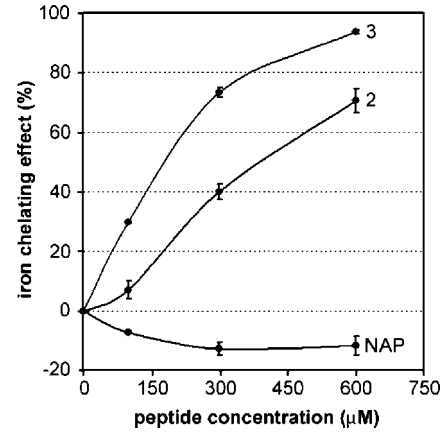

Figure 3. Iron-chelating potency. The chelating effect is expressed as percent of control (60 μM ferrozine, 15 μM $FeSO_4$ in pH 6.9 ammonium acetate buffer). DFO $IC_{50} = 10$ μM. Values represent the mean ± SEM, $n = 3$ in duplicate.

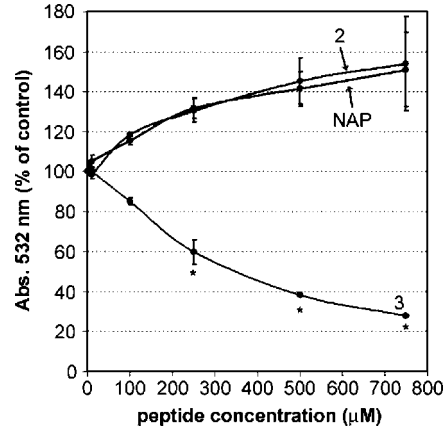

Figure 4. Inhibition of lipid peroxidation. Lipid peroxidation (LPO) was performed in rat brain mitochondrial homogenates. LPO was induced by 1.5 μM $FeSO_4$. Results are expressed as percent of control (no drug). DFO achieved nearly complete inhibition at 15 μM. Values represent the mean ± SEM, $n = 3$ in duplicate: (∗) $P < 0.05$.

was absent from the reaction (not shown). One possible explanation for the unexpected behavior of these peptides is that at high concentrations they may bind iron in a manner that enhances its propensity to participate in electron-transfer reactions. The idea that some chelators increase the redox activity of the bound metals is not a novel one, as it has been previously reported that the commonly used metal chelator EDTA rather stimulates the production of ROS in the presence of iron.[52,53] The NAP sequence includes several potential iron binding moieties, including the amide groups in peptide bonds and on the asparagine and glutamine residues, the hydroxyl group on the serine residue, and the C-terminal carboxyl group. Any of these may be held accountable for binding iron in a redox-competent manner when the peptide is in large excess over the metal. On this account, the possibility that the potency of **3** to inhibit lipid peroxidation is hampered by some intrinsic property of the NAP sequence cannot be excluded, and this may at least partially explain the superior potency exhibited by DFO in this model, establishing nearly complete protection at 15 μM (not shown).

Inhibition of Hydroxyl Radical Formation. It is a well-established concept that one of the principal routes by which hydroxyl radicals are generated in living systems is through the interaction of transition metals, particularly the ferrous ion, with hydrogen peroxide (Fenton reaction). In order to assess the ability of NAP iron chelators to inhibit the Fenton reaction, an electron paramagnetic resonance (EPR) spin trapping method was used. Hydroxyl radicals were produced by mixing H_2O_2 and $FeSO_4$, and the resulting radicals were trapped with the spin trap *N*-phenyl-*tert*-butylnitrone (PBN). The EPR spectrum obtained in the Fenton system in the presence of PBN consisted of a sextet with hyperfine splitting constants of $a_N = 16.1$ G, $a_H = 2.3$ G, typical of PBN−$OH^{\bullet}$ spin adducts in water[54] (Figure 5A). Addition of **3** (600 μM), as well as DFO (300 μM, not shown), caused a marked reduction in the EPR signal intensity to 28% and 12% of control, respectively. In contrast, addition of the native NAP peptide (600 μM) led to a 23% increase in the PBN−$OH^{\bullet}$ spin adduct concentrations, while neither peptides **1** nor **2** showed any significant effect on the EPR signal intensity. These findings were in line with the results of the lipid peroxidation experiments in which native NAP also demonstrated a pro-oxidative effect as opposed to the inhibitory effects of the iron-chelating compounds **3** and DFO. In addition, this behavior of native NAP, together with the fact that the PBN

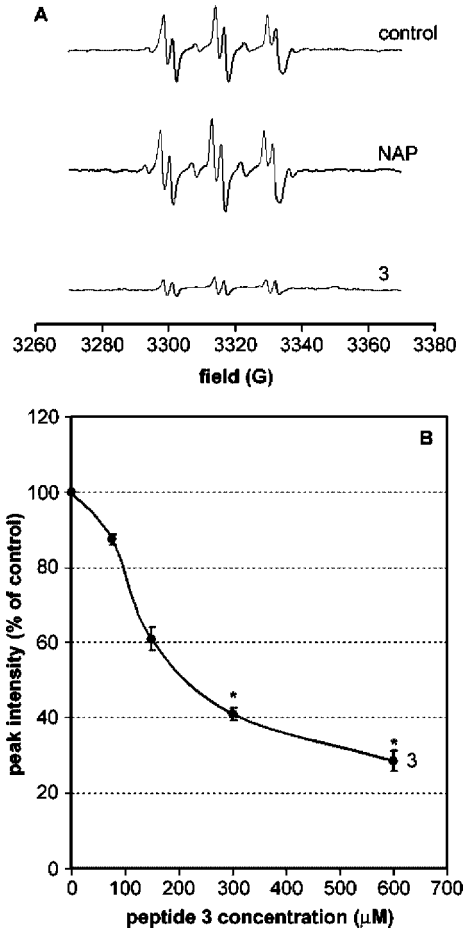

Figure 5. Inhibition of hydroxyl radical generation. (A) Representative EPR spectra of reaction systems containing 100 μM $FeSO_4$, 200 μM H_2O_2, and native NAP or peptide **3** (600 μM) or none (control). Hydroxyl radical generation in the presence of DFO (300 μM) was 12% of control. (B) Concentration-dependence curve for peptide **3**. Results are expressed as percent of control, calculated as the peak intensity of the middle field doublet. Values represent the mean ± SEM, $n = 3$: (*) $P < 0.05$.

spin trap was in at least a ~60-fold excess over the tested compounds, implies that the pronounced decrease in the production of hydroxyl radicals in the presence of **3** can be more likely attributed to its iron-chelating activity rather than to an ability to scavenge the generated radicals.

The inhibitory effect of **3** on the Fenton reaction was found to be concentration-dependent (Figure 5B), with an estimated IC_{50} value of 150 μM (1.5 times the iron concentration). It is mentioned that **3** did not achieve complete inhibition of hydroxyl radical formation at any of the concentrations measured and a minimum of ~20% of EPR spin adduct signal intensity was always detected.

In Vitro Neuroprotection. NAP and peptide **3** were tested for their capacity to protect human SH-SY5Y neuroblastoma cells against oxidative stress-associated death induced by H_2O_2. In this assay, addition of 80 μM H_2O_2 to the growth medium reduced cell viability to 56% compared to control. The tested compounds were added to the medium at different concentrations immediately prior to the H_2O_2 insult. As can be seen in Figure 6, both native NAP and **3** exhibited a neuroprotective effect at concentrations ranging from 1 pM to 10 nM, with **3** showing higher protective capabilities. Neither of the tested peptides showed a toxic effect at concentrations of up to 10^{-5} M (not shown).

The NAP peptide has been reported to possess neuroprotective properties in a wide range of in vitro neurodegeneration models, protecting against a multitude of neurotoxins.[30,32–34] In all these models, NAP has been shown to be most effective at very low concentrations, ranging from 10^{-16} to 10^{-8} M. The mechanism by which NAP exerts neuroprotection is yet to be delineated. To date, it has been shown that NAP interferes with inflammatory processes[55] and modulates signal transduction pathways by inducing cGMP[56] production. In addition, NAP is a promoter of microtubule assembly, another means by which it can enhance cell survival.[57] Most relevant to the present work, NAP has been reported to curtail the overexpression of the key proapoptotic protein p53 following exposure of cell cultures to H_2O_2.[31]

The results of our neuroprotection experiment reaffirm that the NAP peptide can protect against oxidative stress-associated cell death. In addition, our findings suggest that conferment of NAP with iron-binding capabilities enhances its neuroprotective effect, presumably via chelating iron and restraining its redox activity.

Summary and Conclusion

The NAP peptide, whose neuroprotective capabilities have been demonstrated in a multitude of experimental settings, was used in this study as base for the design of novel peptide iron chelators. Three such compounds were synthesized, and their potential to counteract some of the aspects of neurodegeneration were evaluated. Special emphasis was given to examining the effects of these novel peptide chelators on the iron-associated generation of ROS, a concept that has been widely recognized in the past 2 decades as a key pathogenic factor in neurodegenerative disorders. The central involvement of iron in oxidative stress suggests that the strategy of iron chelation may be superior to treatment with antioxidants, since it is aimed at blocking the production of ROS rather than scavenging them.

Despite their ability to bind iron, the monohydroxamate NAP derivatives **1** and **2** were ineffective in quenching the redox activity of this metal, as demonstrated in the lipid peroxidation and EPR assays. In contrast, the dihydroxamate peptide **3** did show a capacity for reducing iron-associated ROS generation. This suggests to us that the number of hydroxamates bound to the iron has critical influence on its capacity to participate in electron-transfer reactions. Spectrophotometric studies, complemented by mass spectrometry, revealed a 1 to 1 (peptide **3** to Fe) ratio in the complex formed under the experimental conditions. In such a complex, four of the six coordinates of the iron are satisfied by **3**'s two hydroxamate groups, while the two other coordinates are probably occupied by water molecules (Scheme 2). In any of the techniques employed, we were not able to detect the formation of a 3 to 2 (peptide **3** to Fe) complex in which all iron coordinates would have been occupied by hydroxamates. It is possible that the lack of formation of such a complex is due to steric hindrance, with side chains of nearby amino acids blocking the access of a hydroxamate group from a second peptide molecule. This may be part of the explanation for the superior potency observed with the trihydroxamate DFO in inhibiting the Fenton reaction and lipid peroxidation, since DFO forms 1:1 complexes with iron, capturing all six coordinates. Occupation of all coordination sites can greatly influence the redox properties, solubility, and biological activity of iron. Graf et al.[52] have shown that the presence of coordinated water or other readily exchangeable ligands correlates with the catalytic activity of the metal-chelator complex and that stable coordination of all six sites results in the inability of iron to catalyze the Fenton reaction. They base this assumption on the

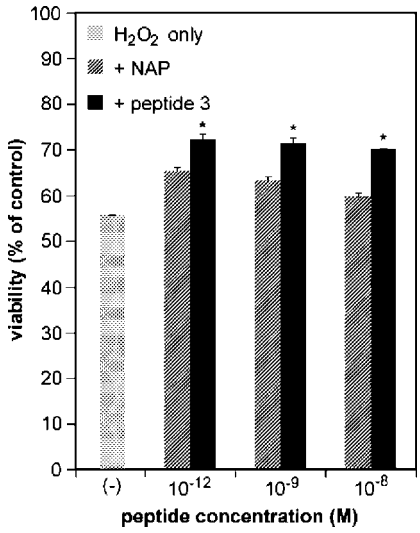

Figure 6. Neuroprotection against H_2O_2 toxicity. NAP and peptide **3** were tested for neuroprotective activity against H_2O_2 toxicity in SH-SY5Y neuroblastoma cell cultures. Results are expressed as percent viability compared to cells not treated with H_2O_2. Viability with DFO at 10^{-6} and 10^{-5} M was 76%. Values represent the mean ± SEM, $n = 7$ in two separate experiments: (*) $P < 0.05$.

Scheme 2. Schematic Representation of Peptide **3**−Fe Complex

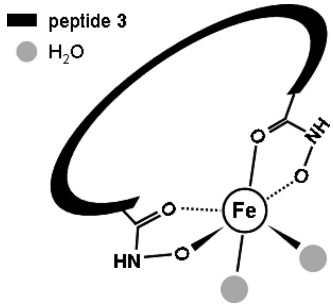

premise that constant cycling of the iron ion between its two oxidation states is an essential requirement for the propagation of the Fenton reaction. According to Graf, the availability of a water coordination site on the ligand−Fe complex is key for the reduction of iron back to Fe(II) to take place;[52] otherwise the iron remains stable in the Fenton-inactive Fe(III) state.

The results obtained with **3** in the neuroprotection assay are of great promise. Not only do they show that **3** can also interfere with oxidative processes in biological systems but they also suggest that it does so in a bifunctional manner. The finding that **3** exerts superior neuroprotection compared to native NAP suggests that its activity can be partially attributed to the chelation of iron.

Finally, it is also tempting to speculate that **3** may possess qualities of targeting toward sites of neurodegeneration. Such targeting may occur on account of the native NAP peptide forming specific interactions with brain proteins such as the brain-specific β-III-tubulin[58] and the Aβ peptide.[30] Moreover, the notion that iron accumulates mostly in sites of neurodegeneration may also enhance the neuroprotective activity arising from the NAP sequence. Thus, the concept of targeting is possibly an additional dimension by which **3** is superior to its parent peptide and may also pose an advantage in comparison to DFO. However, only in vivo studies can demonstrate the validity of these suggestions, and such studies are beyond the scope of the present work.

In conclusion, the promising results obtained with **3** suggest that this line of drug development should be further pursued. Future research should concentrate on attempts to modify **3** in order to further improve its ability to quench iron-associated oxidative stress. A key step in refining **3** may be to find the underlying reason for the intrinsic propensity of the NAP sequence to stimulate ROS generation in the presence of iron. In addition, the prospects of adding a third hydroxamate moiety to the peptide should also be investigated. Naturally, any future modifications will have to be performed in a manner that does not damage the intrinsic neuroprotective qualities of the NAP sequence.

Experimental Section

General. Unless otherwise specified, all chemicals and reagents were of analytical grade and were purchased from Sigma-Aldrich (St. Louis, MO), Merck (Darmstadt, Germany) or Fluka (Buchs, Switzerland). HPLC grade acetonitrile and trifluoracetic acid (TFA) were from JT Baker (Phillipsburg, NJ). Preloaded Wang resins, *N*-α-9-fluorenylmethoxycarbonyl (Fmoc)-protected amino acids and benzotriazol-1-yloxytripyrrolidinophosphonium hexafluorophosphate (PyBOP) were from Novabiochem (Laufelfingen, Switzerland).

Unless otherwise stated, spectrophotometric studies were performed with a Varian Cary 50 UV–visible spectrophotometer (Palo Alto, CA).

All crude peptides were initially screened by analytical reversed-phase high-performance liquid chromatography (HPLC) using an RP-18, 100 mm × 4.6 mm Chromolith column (Merck). Peptide purifications were then performed on a Spectra-Physics SP8800 HPLC system equipped with an Applied Biosystems 757 variable-wavelength absorbance detector that was set to 220 nm. The preparative HPLC prepacked column was Vydac RP-18, 250 mm × 22 mm, bead size 10 μm (Bucher Biotec AG, Basel, Switzerland). Analysis and purification were attained with a binary gradient comprising 0.1% TFA in H_2O (solution A) and 0.1% TFA in 75% aqueous acetonitrile (solution B). Purifications were achieved with a 10–100% B gradient over 50 min with a flow of 10.0 mL/min.

Following purification, all newly synthesized peptides were subjected to amino acid analysis and electron spray ionization mass spectrometry (ESI-MS), performed on a Micromass Platform LCZ 4000 (Manchester, U.K.).

Peptide Synthesis. General Procedure. All peptides were synthesized via the Fmoc strategy[59] either manually or by automatic procedure with an APEX 396 synthesizer (Advanced Chemtech, Louisville, KY). Synthesis scales were between 25 and 100 μmol. Unless otherwise stated, the solid support was Wang resin preloaded with the Fmoc-protected C-terminal amino acid. The resin was swollen for 30 min in *N*-methylpyrrolidone (NMP) prior to the first coupling step. Side chain protecting groups were as follows: Asn(Trt), Ser(tBu), Gln(Trt). PyBOP (2 equiv, 50−200 μmol) with *N*-methylmorpholine (NMM, 4 equiv, 100−400 μmol) and, when necessary, a combination of dicyclohexylcarbodiimide (DCC, 3 equiv, 75−300 μmol) and *N*-hydroxybenzotriazole (HOBt, 3 equiv, 75−300 μmol) were utilized as coupling reagents. Before each coupling step, removal of the α-amino protecting group Fmoc was achieved by shaking in 20% piperidine in DMF. In manual procedures, ninhydrin tests were employed in order to monitor the success of each coupling and deprotection step. Side chain deprotection and cleavage of the peptide from the resin were performed simultaneously using a solution of TFA/triethylsilane/water (90:5:5 v/v) for 2–4 h. The cleavage mixtures were filtered, and the peptides were precipitated from the solution with dry peroxide-free methyl *tert*-butyl ether at 0 °C. The pellets were washed with ether twice more and were then dissolved in water and lyophilized.

Peptide 3 (H_2N-Asp(CONHOH)-Ala-Pro-Val-Ser-Ile-Pro-Gln-CONHOH). Hydroxylamine Wang resin (Bachem, Bubendorf, Switzerland) was shaken for 2 × 90 min with a mixture of Fmoc-

Gln(Trt)-OH (2 equiv, 200 μM), PyBOP (200 μM), and diisopropylethylamine (DIPEA, 400 μM) in DCM (Scheme 1). The coupling solution was drained, and the resin was washed (3 × DCM, 3 × DMF, 2 × DCM) and then dried in vacuo over KOH. For resin loading determination, 1 mg of resin was shaken for 5 min in 3 mL of 20% piperidine in DMF, followed by measurement of the UV absorbance at 290 nm. An estimate of the Gln attachment level was obtained using the equation

$$\text{loading (mmol/g)} = (\text{Abs}_{\text{sample}} - \text{Abs}_{\text{ref}})/[(1.65)(\text{milligrams of resin})]$$

with a solution of 20% piperidine serving as reference. Resin loading was normally 0.7–0.8 mmol/g. Further extension of the peptide was accomplished using standard Fmoc strategy, as described above. Boc-Asp(Ofm)-OH (Bachem) was chosen as the N-terminal amino acid, allowing for the selective removal of the *O*-fluorenylmethyl (OFm) side chain protecting group. This was achieved with 20% piperidine in DMF for 20 and then 40 min. The peptide−resin was then washed (3 × DMF, 3 × DCM) and introduced with *O*-benzylhydroxylamine−HCl (300 μM), PyBOP (300 μM), and NMM (600 μM) in DMF. The mixture was shaken for 120 min, after which the liquid was drained and a second, identical coupling step was performed. A third and final coupling step was performed via DCC/HOBt activation: a mixture of *O*-benzylhydroxylamine−HCl (300 μM), HOBt (300 μM), and DCC (300 μM) in DMF was added to the resin followed by shaking for 18 h. The solution was then drained, and the resin was washed. Peptide cleavage and removal of all protecting groups other than *O*-benzyl were performed with a solution of TFA/triethylsilane (95:5 v/v). Following ether precipitation and washing, removal of the *O*-benzyl group from the modified aspartic acid side chain was performed as follows: the peptide was dissolved in 10 mL of 95% ethanol and 50 mg of 10% Pd/charcoal as catalyst was added. The solution was then stirred in 1 atm of H_2 for 4 h (Scheme 1). The Pd/charcoal powder was filtered out and washed several times with ethanol, and the solvents were evaporated in vacuo to a volume of ~1 mL. Further treatment of the peptide was performed as described above.

In addition to the dihydroxamate peptide **3**, two monohydroxamate peptides were synthesized: peptide **1** (H_2N-Asn-Ala-Pro-Val-Ser-Ile-Pro-Gln-CONHOH) and peptide **2** (H_2N-Asp(CONHOH)-Ala-Pro-Val-Ser-Ile-Pro-Gln-OH). Peptide **1** was synthesized using the standard procedure on hydroxylamine Wang resin, while peptide **2** was synthesized on Wang resin preloaded with Fmoc-Gln(Trt), with the remainder of the synthesis route similar to peptide **3**.

Assessment of Fe(II)-Binding Capacity. The iron-binding capacity of the test compounds was determined by assessing their ability to compete with ferrozine (3-[2-pyridyl]-5,6-diphenyl-1,2,4-triazine-4,4′-disulfonic acid) for ferrous ions, resulting in reduced absorbance of the ferrozine−Fe(II) complex at 562 nm. Reactions were carried out in 5% ammonium acetate buffer (pH 6.9). Various concentrations of the tested compounds (100–600 μM, in duplicate) were incubated with $FeSO_4$ (15 μM) for 30 min, followed by the addition of 60 μM ferrozine (Sigma-Aldrich). After 1 h of incubation at ambient temperature, the absorbance of the resulting solutions at 562 nm was read with a Tecan Sunrise ELISA reader (Lannedorf, Switzerland). Following subtraction of any absorbance by a blank solution, the Fe (II)-chelating effect was calculated as follows:

$$\text{chelating effect (\%)} = [1 - (\text{Abs}_{562\text{nm}} \text{ of sample})/(\text{Abs}_{562\text{nm}} \text{ of control})] \times 100$$

Mitochondria Isolation for Lipid Peroxidation Assay. Mitochondrial membrane homogenates were prepared from rat brains as previously described.[60] Briefly, male Sprague-Dawley rats (250–300 g) were killed by decapitation. The brains were extracted and transferred into ice-cold 10 mM Tris-HCl buffer (pH 7.5) containing 0.25 M sucrose, 2 mM EDTA, and 2% bovine serum albumin. Brains were homogenized separately, and a crude mitochondrial fraction was prepared by differential centrifugation, followed by washing with 10 mM Tris-HCl buffer containing 0.25 M sucrose. The homogenate protein concentration was measured using the Bradford assay.

Lipid Peroxidation Assay. Reactions were carried out in 25 mM Tris-HCl buffer (pH 7.5) containing 25 μM ascorbate. Each reaction mixture (150 μL final volume) contained a mitochondrial preparation equivalent to 40 μg of protein (as determined by the Bradford assay), 1.5 μM $FeSO_4$, and various concentrations of the tested compounds (10–750 μM). The samples were shaken at ambient temperature for 2 h, after which the reaction was terminated by addition of 150 μL of 20% trichloroacetic acid. The samples were centrifuged (10000*g* for 10 min), and 200 μL supernatant was mixed with 200 μL of 0.5% thiobarbituric acid (TBA), followed by heating to 95 °C for 30 min. The absorbance of thiobarbituric acid derivatives was measured photometrically at 532 nm (Tecan Sunrise ELISA reader). Results are expressed as percent of control following subtraction of the absorbance of the blank solution.

Detection of Hydroxyl Radical Formation by EPR. The effect of various compounds on the iron-induced generation of hydroxyl radicals ($^{\bullet}$OH) was tested by the electron paramagnetic resonance (EPR) technique, utilizing phenyl-*tert*-butylnitrone (PBN) as the spin trap. PBN−OH$^{\bullet}$ spin adducts were obtained from a Fenton reaction system that contained 100 μM $FeSO_4$, 200 μM H_2O_2, and 35 mM PBN. The tested compounds were added 2 min prior to the addition of H_2O_2. The mixture was then immediately transferred into a quartz flat cell (60 μM), and the EPR spectrum was recorded in an ELEXYS 500 spectrometer (Bruker, Karlsruhe, Germany) at room temperature. The standard instrumental parameters were as follows: microwave frequency 9.34 GHz; microwave power 39.9 mW; center of field 3320 G; modulation amplitude 1 G; scan range 100 G; time constant 1.31 s; and constant receiver gain. The EPR spectrum of the PBN−OH$^{\bullet}$ spin adduct consisted of a sextet with hyperfine splitting constants of $a_N = 16.1$ G, $a_H = 2.3$ G. The peak intensity of the middle field doublet was taken as an estimation of the concentration of the spin adducts generated.

Cell Cultures and Treatment. Human SH-SY5Y neuroblastoma cells were grown at 37 °C in a humid 5% CO_2, 95% air environment. The growth medium comprised a 1:1 mixture of Eagle's minimum essential medium (Eagle MEM) and Ham's F-12 medium (Invitrogen, Groningen, The Netherlands), supplemented with 10% fetal calf serum (FCS, Beit Haemek, Israel), 1 mM sodium pyruvate, 2% sodium bicarbonate, and 1% of a mixture of penicillin−streptomycin−nystatin. When cells reached the required confluence, the culture medium was removed and the cells were detached by vigorous washing followed by centrifugation at 200*g* for 5 min. The cells were then counted, diluted in their growth medium to the desired titer, and transferred into 96-well microtiter plates (100 μL medium containing 0.5×10^4 cells per well). The cells were allowed to attach for 24 h prior to the addition of the tested compounds or vehicle, followed by immediate insults with H_2O_2 (80 μM). The cells were incubated at 37 °C for 24 h before being assayed with MTT.

MTT Assay for Cell Viability. This assay is based on the reduction of 3-(4,5-dimethylthiazol-2-yl)-2,5-diphenyltetrazolium bromide (MTT) to blue formazan crystals by mitochondrial dehydrogenases, which are active only in living cells.[61] The medium was removed 24 h after treatment and replaced with fresh medium (100 μM/well). To each well, 10 μL of a 5 mg/mL MTT solution in PBS was added. Following incubation at 37 °C for 2 h, 100 μL of 10% SDS in 0.01 N HCl was added and the plates were incubated for additional 24 h. Absorbance was determined in a Tecan Sunrise ELISA reader at 570 nm/650 nm after automatic subtraction of background readings. Results are expressed as percent viability compared to untreated cells.

Statistical Analysis. Where relevant, the data in the figures are expressed as the mean ± SEM. Statistical analyses were performed by using ANOVA followed by Dunnett's test to compare each treatment against control. Variations were considered statistically significant for $P < 0.05$.

Acknowledgment. We thank Sara Rubinraut for synthesizing some of the peptides, and Orit Bar-Am and Shunit Gal for technical assistance. Mati Fridkin is the Lester Pearson Professor of Protein Chemistry.

References

(1) Barnham, K. J.; Masters, C. L.; Bush, A. I. Neurodegenerative Diseases and Oxidative Stress. *Nat. Rev. Drug Discovery* **2004**, *3*, 205–214.

(2) Soto, C. Unfolding the Role of Protein Misfolding in Neurodegenerative Diseases. *Nat. Rev. Neurosci.* **2003**, *4*, 49–60.

(3) Montine, T. J.; Neely, M. D.; Quinn, J. F.; Beal, M. F.; Markesbery, W. R.; Roberts, L. J.; Morrow, J. D. Lipid Peroxidation in Aging Brain and Alzheimer's Disease. *Free Radical Biol. Med.* **2002**, *33*, 620–626.

(4) Dexter, D. T.; Carter, C. J.; Wells, F. R.; Javoy-Agid, F.; Agid, Y.; Lees, A.; Jenner, P.; Marsden, C. D. Basal Lipid Peroxidation in Substantia Nigra Is Increased in Parkinson's Disease. *J. Neurochem.* **1989**, *52*, 381–389.

(5) Butterfield, D. A.; Lauderback, C. M. Lipid Peroxidation and Protein Oxidation in Alzheimer's Disease Brain: Potential Causes and Consequences Involving Amyloid Beta-Peptide-Associated Free Radical Oxidative Stress. *Free Radical Biol. Med.* **2002**, *32*, 1050–1060.

(6) Gabbita, S. P.; Lovell, M. A.; Markesbery, W. R. Increased Nuclear DNA Oxidation in the Brain in Alzheimer's Disease. *J. Neurochem.* **1998**, *71*, 2034–2040.

(7) Alam, Z. I.; Jenner, A.; Daniel, S. E.; Lees, A. J.; Cairns, N.; Marsden, C. D.; Jenner, P.; Halliwell, B. Oxidative DNA Damage in the Parkinsonian Brain: An Apparent Selective Increase in 8-Hydroxyguanine Levels in Substantia Nigra. *J. Neurochem.* **1997**, *69*, 1196–1203.

(8) Zecca, L.; Youdim, M. B.; Riederer, P.; Connor, J. R.; Crichton, R. R. Iron, Brain Ageing and Neurodegenerative Disorders. *Nat. Rev. Neurosci.* **2004**, *5*, 863–873.

(9) Morita, A.; Kimura, M.; Itokawa, Y. The Effect of Aging on the Mineral Status of Female Mice. *Biol. Trace Elem. Res.* **1994**, *42*, 165–177.

(10) Takahashi, S.; Takahashi, I.; Sato, H.; Kubota, Y.; Yoshida, S.; Muramatsu, Y. Age-Related Changes in the Concentrations of Major and Trace Elements in the Brain of Rats and Mice. *Biol. Trace Elem. Res.* **2001**, *80*, 145–158.

(11) Lovell, M. A.; Robertson, J. D.; Teesdale, W. J.; Campbell, J. L.; Markesbery, W. R. Copper, Iron and Zinc in Alzheimer's Disease Senile Plaques. *J. Neurol. Sci.* **1998**, *158*, 47–52.

(12) Smith, M. A.; Harris, P. L.; Sayre, L. M.; Perry, G. Iron Accumulation in Alzheimer Disease Is a Source of Redox-Generated Free Radicals. *Proc. Natl. Acad. Sci. U.S.A.* **1997**, *94*, 9866–9868.

(13) Castellani, R. J.; Siedlak, S. L.; Perry, G.; Smith, M. A. Sequestration of Iron by Lewy Bodies in Parkinson's Disease. Acta. *Neuropathology (Berlin)* **2000**, *100*, 111–114.

(14) Wardman, P.; Candeias, L. P. Fenton Chemistry: An Introduction. *Radiat. Res.* **1996**, *145*, 523–531.

(15) Tabner, B. J.; Turnbull, S.; El-Agnaf, O. M.; Allsop, D. Formation of Hydrogen Peroxide and Hydroxyl Radicals from A(Beta) and Alpha-Synuclein as a Possible Mechanism of Cell Death in Alzheimer's Disease and Parkinson's Disease. *Free Radical Biol. Med.* **2002**, *32*, 1076–1083.

(16) Huang, X.; Atwood, C. S.; Hartshorn, M. A.; Multhaup, G.; Goldstein, L. E.; Scarpa, R. C.; Cuajungco, M. P.; Gray, D. N.; Lim, J.; Moir, R. D.; Tanzi, R. E.; Bush, A. I. The A Beta Peptide of Alzheimer's Disease Directly Produces Hydrogen Peroxide through Metal Ion Reduction. *Biochemistry* **1999**, *38*, 7609–7616.

(17) Turnbull, S.; Tabner, B. J.; El-Agnaf, O. M.; Moore, S.; Davies, Y.; Allsop, D. Alpha-Synuclein Implicated in Parkinson's Disease Catalyses the Formation of Hydrogen Peroxide in Vitro. *Free Radical Biol. Med.* **2001**, *30*, 1163–1170.

(18) Mantyh, P. W.; Ghilardi, J. R.; Rogers, S.; DeMaster, E.; Allen, C. J.; Stimson, E. R.; Maggio, J. E. Aluminum, Iron, and Zinc Ions Promote Aggregation of Physiological Concentrations of Beta-Amyloid Peptide. *J. Neurochem.* **1993**, *61*, 1171–1174.

(19) Hu, W. P.; Chang, G. L.; Chen, S. J.; Kuo, Y. M. Kinetic Analysis of Beta-Amyloid Peptide Aggregation Induced by Metal Ions Based on Surface Plasmon Resonance Biosensing. *J. Neurosci. Methods.* **2006**, *154*, 190–197.

(20) Uversky, V. N.; Li, J.; Fink, A. L. Metal-Triggered Structural Transformations, Aggregation, and Fibrillation of Human Alpha-Synuclein. A Possible Molecular Link between Parkinson's Disease and Heavy Metal Exposure. *J. Biol. Chem.* **2001**, *276*, 44284–44296.

(21) Rogers, J. T.; Randall, J. D.; Cahill, C. M.; Eder, P. S.; Huang, X.; Gunshin, H.; Leiter, L.; McPhee, J.; Sarang, S. S.; Utsuki, T.; Greig, N. H.; Lahiri, D. K.; Tanzi, R. E.; Bush, A. I.; Giordano, T.; Gullans, S. R. An Iron-Responsive Element Type II in the 5′-Untranslated Region of the Alzheimer's Amyloid Precursor Protein Transcript. *J. Biol. Chem.* **2002**, *277*, 45518–45528.

(22) Ben-Shachar, D.; Eshel, G.; Finberg, J. P.; Youdim, M. B. The Iron Chelator Desferrioxamine (Desferal) Retards 6-Hydroxydopamine-Induced Degeneration of Nigrostriatal Dopamine Neurons. *J Neurochem.* **1991**, *56*, 1441–1444.

(23) Lan, J.; Jiang, D. H. Desferrioxamine and Vitamin E Protect against Iron and MPTP-Induced Neurodegeneration in Mice. *J. Neural Transm.* **1997**, *104*, 469–481.

(24) Kaur, D.; Yantiri, F.; Rajagopalan, S.; Kumar, J.; Mo, J. Q.; Boonplueang, R.; Viswanath, V.; Jacobs, R.; Yang, L.; Beal, M. F.; DiMonte, D.; Volitaskis, I.; Ellerby, L.; Cherny, R. A.; Bush, A. I.; Andersen, J. K. Genetic or Pharmacological Iron Chelation Prevents Mptp-Induced Neurotoxicity in Vivo: A Novel Therapy for Parkinson's Disease. *Neuron* **2003**, *37*, 899–909.

(25) Cherny, R. A.; Atwood, C. S.; Xilinas, M. E.; Gray, D. N.; Jones, W. D.; McLean, C. A.; Barnham, K. J.; Volitakis, I.; Fraser, F. W.; Kim, Y.; Huang, X.; Goldstein, L. E.; Moir, R. D.; Lim, J. T.; Beyreuther, K.; Zheng, H.; Tanzi, R. E.; Masters, C. L.; Bush, A. I. Treatment with a Copper−Zinc Chelator Markedly and Rapidly Inhibits Beta-Amyloid Accumulation in Alzheimer's Disease Transgenic Mice. *Neuron* **2001**, *30*, 665–676.

(26) Whitnall, M.; Richardson, D. R. Iron: A New Target for Pharmacological Intervention in Neurodegenerative Diseases. *Semin. Pediatr. Neurol.* **2006**, *13*, 186–197.

(27) Shachar, D. B.; Kahana, N.; Kampel, V.; Warshawsky, A.; Youdim, M. B. Neuroprotection by a Novel Brain Permeable Iron Chelator, Vk-28, against 6-Hydroxydopamine Lession in Rats. *Neuropharmacology* **2004**, *46*, 254–263.

(28) Levites, Y.; Weinreb, O.; Maor, G.; Youdim, M. B.; Mandel, S. Green Tea Polyphenol (−)-Epigallocatechin-3-Gallate Prevents *N*-Methyl-4-phenyl-1,2,3,6-tetrahydropyridine-Induced Dopaminergic Neurodegeneration. *J. Neurochem.* **2001**, *78*, 1073–1082.

(29) Reznichenko, L.; Amit, T.; Zheng, H.; Avramovich-Tirosh, Y.; Youdim, M. B.; Weinreb, O.; Mandel, S. Reduction of Iron-Regulated Amyloid Precursor Protein and Beta-Amyloid Peptide by (−)-Epigallocatechin-3-Gallate in Cell Cultures: Implications for Iron Chelation in Alzheimer's Disease. *J. Neurochem.* **2006**, *97*, 527–536.

(30) Ashur-Fabian, O.; Segal-Ruder, Y.; Skutelsky, E.; Brenneman, D. E.; Steingart, R. A.; Giladi, E.; Gozes, I. The Neuroprotective Peptide NAP Inhibits the Aggregation of the Beta-Amyloid Peptide. *Peptides* **2003**, *24*, 1413–1423.

(31) Gozes, I.; Steingart, R. A.; Spier, A. D. NAP Mechanisms of Neuroprotection. *J. Mol. Neurosci.* **2004**, *24*, 67–72.

(32) Bassan, M.; Zamostiano, R.; Davidson, A.; Pinhasov, A.; Giladi, E.; Perl, O.; Bassan, H.; Blat, C.; Gibney, G.; Glazner, G.; Brenneman, D. E.; Gozes, I. Complete Sequence of a Novel Protein Containing a Femtomolar-Activity-Dependent Neuroprotective Peptide. *J. Neurochem.* **1999**, *72*, 1283–1293.

(33) Steingart, R. A.; Solomon, B.; Brenneman, D. E.; Fridkin, M.; Gozes, I. VIP and Peptides Related to Activity-Dependent Neurotrophic Factor Protect PC12 Cells against Oxidative Stress. *J. Mol. Neurosci.* **2000**, *15*, 137–145.

(34) Offen, D.; Sherki, Y.; Melamed, E.; Fridkin, M.; Brenneman, D. E.; Gozes, I. Vasoactive Intestinal Peptide (VIP) Prevents Neurotoxicity in Neuronal Cultures: Relevance to Neuroprotection in Parkinson's Disease. *Brain Res.* **2000**, *854*, 257–262.

(35) Gozes, I.; Giladi, E.; Pinhasov, A.; Bardea, A.; Brenneman, D. E. Activity-Dependent Neurotrophic Factor: Intranasal Administration of Femtomolar-Acting Peptides Improve Performance in a Water Maze. *J. Pharmacol. Exp. Ther.* **2000**, *293*, 1091–1098.

(36) Leker, R. R.; Teichner, A.; Grigoriadis, N.; Ovadia, H.; Brenneman, D. E.; Fridkin, M.; Giladi, E.; Romano, J.; Gozes, I. NAP, a Femtomolar-Acting Peptide, Protects the Brain against Ischemic Injury by Reducing Apoptotic Death. *Stroke* **2002**, *33*, 1085–1092.

(37) Youdim, M. B.; Fridkin, M.; Zheng, H. Bifunctional Drug Derivatives of MAO-B Inhibitor Rasagiline and Iron Chelator Vk-28 as a More Effective Approach to Treatment of Brain Ageing and Ageing Neurodegenerative Diseases. *Mech. Ageing Dev.* **2005**, *126*, 317–326.

(38) Yogev-Falach, M.; Bar-Am, O.; Amit, T.; Weinreb, O.; Youdim, M. B. A Multifunctional, Neuroprotective Drug, Ladostigil (Tv3326), Regulates Holo-APP Translation and Processing. *FASEB J.* **2006**, *20*, 2177–2179.

(39) Zheng, H.; Blat, D.; Fridkin, M.; Novel. Neuroprotective Neurotrophic NAP Analogs Targeting Metal Toxicity and Oxidative Stress: Potential Candidates for the Control of Neurodegenerative Diseases. *J. Neural Transm., Suppl.* **2006**, *71*, 163–172.

(40) Bergeron, R. J.; Wiegand, J.; McManis, J. S.; Perumal, P. T. Synthesis and Biological Evaluation of Hydroxamate-Based Iron Chelators. *J. Med. Chem.* **1991**, *34*, 3182–3187.

(41) Ye, Y.; Liu, M.; Kao, J. L.; Marshall, G. R. Peptide-Bond Modification for Metal Coordination: Peptides Containing Two Hydroxamate Groups. *Biopolymers* **2003**, *71*, 489–515.
(42) Gaeta, A.; Hider, R. C. The Crucial Role of Metal Ions in Neurodegeneration: The Basis for a Promising Therapeutic Strategy. *Br. J. Pharmacol.* **2005**, *146*, 1041–1059.
(43) Harris, D. C.; Aisen, P. Facilitation of Fe(II) Autoxidation by Fe(III) Complexing Agents. *Biochim. Biophys. Acta* **1973**, *329*, 156–158.
(44) Farkas, E.; Enyedy, E. A.; Zekany, L.; Deak, G. Interaction between Iron(II) and Hydroxamic Acids: Oxidation of Iron(II) to Iron(III) by Desferrioxamine B under Anaerobic Conditions. *J. Inorg. Biochem.* **2001**, *83*, 107–114.
(45) Wilkemeyer, M. F.; Chen, S. Y.; Menkari, C. E.; Brenneman, D. E.; Sulik, K. K.; Charness, M. E. Differential Effects of Ethanol Antagonism and Neuroprotection in Peptide Fragment NAPVSIPQ Prevention of Ethanol-Induced Developmental Toxicity. *Proc. Natl. Acad. Sci. U.S.A.* **2003**, *100*, 8543–8548.
(46) Carter, P. Spectrophotometric Determination of Serum Iron at the Submicrogram Level with a New Reagent (Ferrozine). *Anal. Biochem.* **1971**, *40*, 450–458.
(47) Anderegg, G.; L'Eplattenier, F.; Schwarzenbach, G. Hydroxamate Complexes. III. Iron(III) Exchange between Sideramines and Complexones. A Discussion of the Formation Constants of the Hydroxamate Complexes. *Helv. Chim. Acta* **1963**, *46*, 1409–1422.
(48) Spasojevic, I.; Crumbliss, A. L. pH Induced Active ("Uphill") Liquid Membrane Transport of Ferrioxamine B by the Ionizable Ionophore Lasalocid. *Inorg. Chem.* **1999**, *38*, 3248–3250.
(49) Boukhalfa, H.; Crumbliss, A. L. Chemical Aspects of Siderophore Mediated Iron Transport. *BioMetals* **2002**, *15*, 325–339.
(50) Kretchmar Nguyen, S. A.; Craig, A.; Raymond, K. N. Transferrin: The Role of Conformational Changes in Iron Removal by Chelators. *J. Am. Chem. Soc.* **1993**, *115*, 6758–6764.
(51) Singh, S.; Khodr, H.; Taylor, M. I.; Hider, R. C. Therapeutic Iron Chelators and Their Potential Side-Effects. *Biochem. Soc. Symp.* **1995**, *61*, 127–137.
(52) Graf, E.; Mahoney, J. R.; Bryant, R. G.; Eaton, J. W. Iron-Catalyzed Hydroxyl Radical Formation. Stringent Requirement for Free Iron Coordination Site. *J. Biol. Chem.* **1984**, *259*, 3620–3624.
(53) Snyrychova, I.; Pospisil, P.; Naus, J. The Effect of Metal Chelators on the Production of Hydroxyl Radicals in Thylakoids. *Photosynth. Res.* **2006**, *88*, 323–329.
(54) Buettner, G. R. Spin Trapping: ESR Parameters of Spin Adducts. *Free Radical Biol. Med.* **1987**, *3*, 259–303.
(55) Beni-Adani, L.; Gozes, I.; Cohen, Y.; Assaf, Y.; Steingart, R. A.; Brenneman, D. E.; Eizenberg, O.; Trembolver, V.; Shohami, E. A Peptide Derived from Activity-Dependent Neuroprotective Protein (ADNP) Ameliorates Injury Response in Closed Head Injury in Mice. *J. Pharmacol. Exp. Ther.* **2001**, *296*, 57–63.
(56) Ashur-Fabian, O.; Giladi, E.; Furman, S.; Steingart, R. A.; Wollman, Y.; Fridkin, M.; Brenneman, D. E.; Gozes, I. Vasoactive Intestinal Peptide and Related Molecules Induce Nitrite Accumulation in the Extracellular Milieu of Rat Cerebral Cortical Cultures. *Neurosci. Lett.* **2001**, *307*, 167–170.
(57) Gozes, I.; Divinski, I. The Femtomolar-Acting NAP Interacts with Microtubules: Novel Aspects of Astrocyte Protection. *J. Alzheimer's Dis.* **2004**, *6*, S37–S41.
(58) Divinski, I.; Holtser-Cochav, M.; Vulih-Schultzman, I.; Steingart, R. A.; Gozes, I. Peptide Neuroprotection through Specific Interaction with Brain Tubulin. *J. Neurochem.* **2006**, *98*, 973–984.
(59) Atherton, E.; Sheppard, R. C. *Solid Phase Peptide Synthesis: A Practical Approach*; IRL Press: Oxford, U.K., 1989.
(60) Gassen, M.; Glinka, Y.; Pinchasi, B.; Youdim, M. B. Apomorphine Is a Highly Potent Free Radical Scavenger in Rat Brain Mitochondrial Fraction. *Eur. J. Pharmacol.* **1996**, *308*, 219–225.
(61) Hansen, M. B.; Nielsen, S. E.; Berg, K. Re-Examination and Further Development of a Precise and Rapid Dye Method for Measuring Cell Growth/Cell Kill. *J. Immunol. Methods* **1989**, *119*, 203–210.

JM070800L